BILINGUAL PUBLISHING GROUP

Journal of Geographical Research

https://journals.bilpubgroup.com/index.php/jgr

ARTICLE

Application of Vegetation Indices for Detection and Monitoring Oil Spills in Ahoada West Local Government Area of Rivers State, Nigeria

Jonathan Lisa Erebi* , ***Egirani E. Davidson***

Department of Geology, Niger Delta University, Wilberforce Island, Bayelsa State, 560103, Nigeria

ABSTRACT

The study evaluated the environmental effects of an oil spill in Joinkrama 4 and Akimima Ahoada West LGA, Rivers State, Nigeria, using various vegetation indices. Location data for the spill were obtained from the Nigeria Oil Spill Detection and Response Agency, and Landsat imagery was acquired from the United States Geological Survey. Three soil samples were collected from the affected area, and their analysis included measuring total petroleum hydrocarbons (TPH), total hydrocarbons (THC), and polycyclic aromatic hydrocarbons (PAH). The obtained data were processed with ArcGIS software, utilizing different vegetation indices such as the Normalized Difference Vegetation Index (NDVI), Atmospheric Resistant Vegetation Index (ARVI), Soil Adjusted Vegetation Index (SAVI), Green Short Wave Infrared (GSWIR), and Green Near Infrared (GNIR). Statistical analysis was performed using SPSS and Microsoft Excel. The results consistently indicated a negative impact on the environment resulting from the oil spill. A comparison of spectral reflectance values between the oil spill site and the non-oil spill site showed lower values at the oil spill site across all vegetation indices (NDVI 0.0665-0.2622, ARVI –0.0495-0.1268, SAVI 0.0333-0.1311, GSWIR –0.183-0.0517, GNIR –0.0104-–0.1980), indicating damage to vegetation. Additionally, the study examined the correlation between vegetation indices and environmental parameters associated with the oil spill, revealing significant relationships with TPH, THC, and PAH. A t-test with a significance level of $p < 0.05$ indicated significantly higher vegetation index values at the non-oil spill site compared to the oil spill site, suggesting a potential disparity in vegetation health between the two areas. Hence, this study emphasizes the harmful effect of oil spills on vegetation and highlights the importance of utilizing vegetation indices and spectral reflectance analysis to detect and monitor the impact of oil spills on vegetation.

Keywords: Vegetation indices; TPH; PAH; THC; Oil spill; Impact; Rivers State; Nigeria

*CORRESPONDING AUTHOR:

Jonathan Lisa Erebi, Department of Geology, Niger Delta University, Wilberforce Island, Bayelsa State, 560103, Nigeria; Email: jonathanlisa788@gmail.com

ARTICLE INFO

Received: 28 June 2023 | Revised: 27 July 2023 | Accepted: 1 August 2023 | Published Online: 7 August 2023

DOI: https://doi.org/10.30564/jgr.v6i3.5817

CITATION

Erebi, J.L., Davidson, E.E., 2023. Application of Vegetation Indices for Detection and Monitoring Oil Spills in Ahoada West Local Government Area of Rivers State, Nigeria. Journal of Geographical Research. 6(3): 29-41. DOI: https://doi.org/10.30564/jgr.v6i3.5817

1. Introduction

Oil spills in the Niger Delta, particularly in Joinkrama 4 and Akinima, have emerged as a critical global issue with far-reaching consequences for ecosystems, wildlife, and human livelihoods [1] The discovery of crude oil in Oloibiri in 1956 marked the beginning of a series of oil spill incidents, both intentional and unintentional, which have led to the devastation of rivers, seas, and marshes, posing significant environmental hazards [2]. The Niger Delta, acknowledged as one of the world's ten most important wetlands and marine ecosystems, has suffered extensive environmental ramifications due to the presence of numerous oil industries [3]. While these industries have contributed to the growth and development of the region, they have also resulted in adverse impacts. The relentless activities of restless youths who vandalize pipelines and the rising number of illegal refineries in oil-producing areas have substantially amplified environmental contamination [1]. The sensitivity of vegetation to hydrocarbons varies depending on the type and quantity of chemicals involved, as well as the type of vegetation [4]. The impact of oil spills poses a significant threat to the environment in Nigeria, especially in the Niger Delta. If not effectively managed, it could lead to the complete destruction of ecosystems in the region where oil spills have become alarmingly frequent [5]. Communities in this area suffer from the degrading effects of oil spills, as the once-vibrant mangroves that provided fuelwood and habitat for biodiversity have been depleted and rendered lifeless due to oil toxicity. Marine life has also been adversely affected by oil spills, resulting in contaminated seafood and subsequent health risks associated with human consumption. The oil leak has had a significant influence on the health, social, and economic aspects of the affected communities, emphasizing the importance of effective steps to avoid and handle oil disasters in Nigeria's Niger Delta region [6]. Farmlands and sources of potable water are destroyed, further impacting coastal fishing activities. The recurrent incidents of oil spills in the Niger Delta have created significant tension between the local population and multinational oil companies operating in the region. Technological advancements, particularly vegetation spectral indices and remote sensing, offer valuable tools for detecting and monitoring the impacts of oil spills in these environments [7]. Remote sensing techniques, including vegetation spectral indices, have proven effective in detecting and monitoring the effects of hydrocarbon leaks on vegetation health [8]. Changes in leaves, stems, and trunks serve as indicators of plant responses to oil contamination or stress [9]. Continuous monitoring of pipelines and oil leaks at oil production sites is crucial to mitigate oil contamination in rivers, seas, oceans, and marshes.

2. Material and methods

2.1 Location of the study area

The research focuses on the settlements of Joinkrama 4 and Akinima in Rivers State, Nigeria's Ahoada West Local Government Area. These towns are located on the eastern bank of the Orashi River, a significant Niger Delta river (**Figure 1**). Joinkrama 4 is located at roughly 4.8265° N, 6.0665° E, whereas Akinima is located at approximately 5.1046° N, 6.4529° E. The area's geographical location is largely flat, with heights varying from below sea level in the southwest to roughly 39 meters inland [10]. The region is easily accessible by road and footpath, and it has multiple hydrocarbon flow stations operated by Shell Petroleum Development Company (SPDC) and Nigeria Agip Oil Company (NAOC) [10]. The region is drained by various tributaries and creeks, including Kolo Creek and Taylor Creek, which are connected to the Orashi River.

2.2 The geology of the area

The research area is geologically located on the south-western side of the Niger Delta region, which was produced by a failed rift junction between the South American and African plates. The rifting occurred between the late Jurassic and mid-Cretaceous periods [11]. The Niger Delta Basin has an area of more than 105,000 km^2 [12]. The Akata For-

mation, Agbada Formation, and Benin Formation are among the geological formations studied in the area. According to Short and Stauble [13], the Akata Formation, which ranges in age from the Paleocene to the Holocene, is the Niger Delta region's base lithostratigraphic unit. It is made up of thick shales, turbidite sands, and traces of silt and clay. Near the interface with the underlying Agbada Formation, the formation comprises high-pressure, low-density deep marine deposits containing plant remains. It has a varied microfauna, with planktonic foraminifera accounting for a sizable percentage, indicating a shallow maritime shelf depositional environment [14]. The sand and silt streaks inside the formation provide evidence of high-energy deposition as the delta moved into the sea. The Akata Formation extends in thickness from 0 to 6,000 meters and is mostly underwater, not visible at the seashore [15].

2.3 Data collection for oil spill

The satellite data were collected from the United States Geological Survey (USGS). The data includes Landsat-5 acquired on September 12, 1990, with a spatial resolution of 30 meters, and Landsat-8 acquired on December 12, 2021, with a similar spatial resolution. The source for both datasets is the USGS Earth Explorer website. Additionally, oil spill records and corresponding GPS locations from November 2020 to April 2021 were obtained from the Nigeria Oil Spill Detection and Response Agency (NOSDRA) archives, available at https://oilspillmonitor.ng/#/.

2.4 Collection of data for soil

A total number of three (3) soil samples were collected with the aid of a hand auger two were collect-

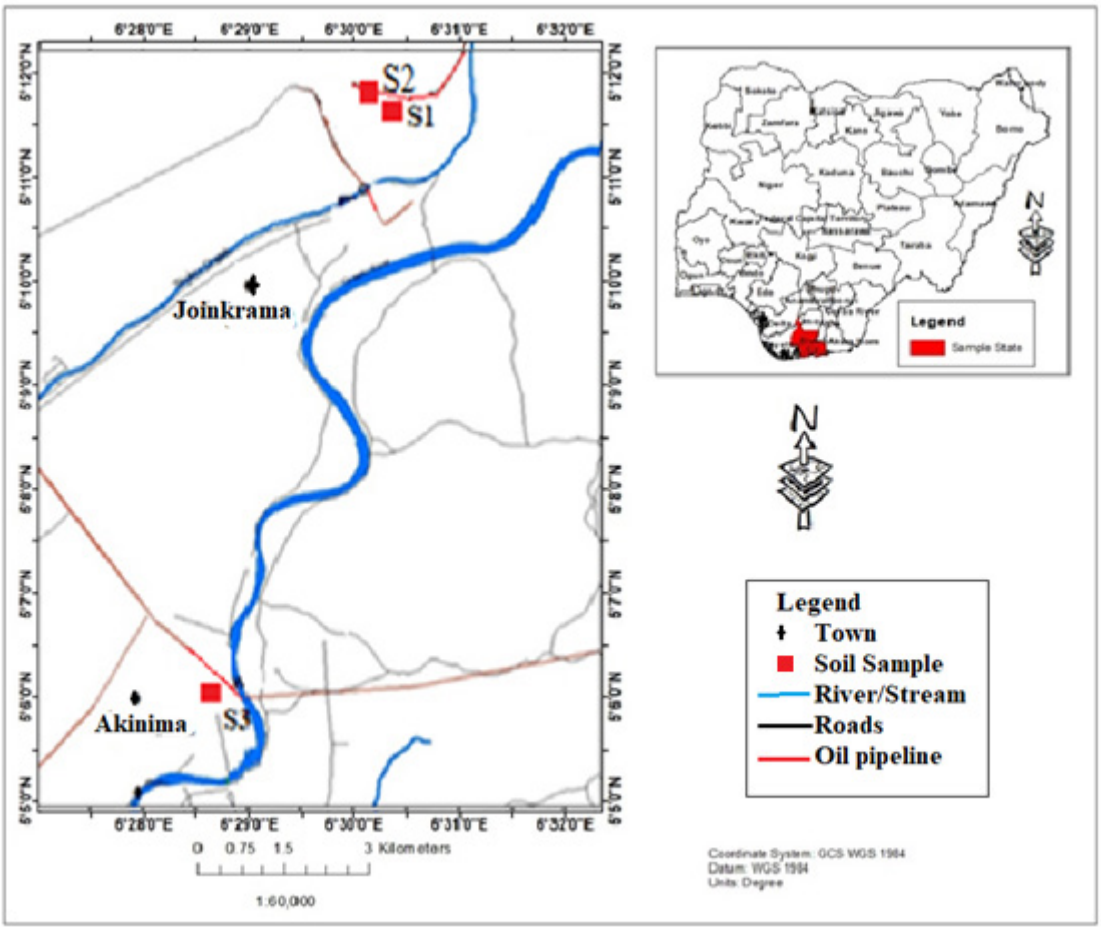

Figure 1. Study area map.

ed in Joinkrama 4, one in Akinima and Soil samples were collected from the outer surface and were analyzed in the laboratory for Polycyclic Aromatic Hydrocarbon, (PAHs), Total Petroleum Hydrocarbons (TPH) and Total Hydrocarbon Content (THC).

2.5 Limitation

In order to minimize the effect of cloud cover, in Landsat-8, this study is limited to the month of December 2021 as there is less cloud cover at this time of the year.

2.6 Data analysis/processing

PAH chemicals were analyzed using gas chromatography, TPH and phenol were measured using a photometer, and THC content was determined through spectrophotometer readings. These analytical techniques and instruments allowed for the accurate identification and quantification of these hydrocarbon compounds in various samples.

The oil spill data was in degrees, minutes and seconds and was imported into Microsoft Excel and converted to degree decimal before it was loaded into the Geographical Information System environment in Database Format to produce a sample location map using Arc GIS software. The Arc GIS spatial analyst extension was used to generate the thematic maps using Map Algebra in a raster calculator, and various vegetation indexes such as NDVI, SAVI, ARVI2, G-NIR and G-SWIR were derived. Finally, SPSS (Statistical Package for the Social Science) and IBM were used for statistical analysis such as Pearson correlation coefficient and T-test were done and Microsoft Excel was also used to plot the bar.

2.7 Vegetation indices

The use of Landsat imagery, specifically Landsat-5 and Landsat-8, is crucial for detecting oil spills and understanding their environmental impact through vegetation indices derived from broadband multispectral data. Five vegetation stress factors are employed in the study, utilizing the spectral bands of Landsat-5 and Landsat-8. For Landsat-8, the spectral bands used for vegetation indices are as follows: visible blue (0.450 to 0.515 μm), visible green (0.525 to 0.6 μm), visible red (0.630 to 0.68 μm), near-infrared (0.845 to 0.885 μm), and short-wave infrared I (1.56 to 1.66 μm), all with a resolution of 30 meters. In the case of Landsat-5, the vegetation indices are derived from the following spectral bands: visible blue (0.450 to 0.515 μm), visible green (0.525 to 0.6 μm), visible red (0.630 to 0.69 μm), near-infrared (0.77 to 0.90 μm), and short-wave infrared 1 (1.55 to 1.75 μm), also with a resolution of 30 meters. By analyzing these vegetation indices derived from Landsat imagery, researchers can assess the extent of oil spills and their impact on the environment, providing valuable insights for environmental studies.

Atmospheric correction refers to the process of adjusting the recorded satellite imagery to account for atmospheric effects and obtain accurate measurements of the Earth's surface. The equations for atmospheric correction of Landsat-8 imager from Digital Number (DN) to Top of Atmosphere (TOA) reflectance using reflectance rescaling coefficients from Landsat-8 metadata file are provided in Equations (1) and (2) [16-18].

Equation (1): TOA reflectance without correction for solar angle (ρλ') can be calculated using the formula:

$$p\lambda = MpQcal + Ap \quad (1)$$

Here, pλ represents TOA planetary reflectance, Mp is the band-specific multiplicative rescaling factor, Aρ is the band-specific additive rescaling factor, and Qcal refers to the quantized and calibrated standard product pixel values (DN).

Equation (2): TOA reflectance corrected for the sun angle can be calculated as follows:

$$p\lambda = (p\lambda) / \cos(\theta sz) = (p\lambda) / \cos(\theta se) \quad (2)$$

In Equation (2), θsz represents the solar zenith angle, while θse represents the solar elevation angle.

The Normalized Difference Vegetation Index (NDVI) is a commonly used spectral index that exhibits distinct characteristics for detecting vegetation stress. It utilizes the red band in the visible spectrum,

which is sensitive to chlorophyll content, and the near-infrared (NIR) band, which indicates healthy vegetation conditions. Equation (3) represents the calculation for NDVI [19,20].

$$NDVI = (RNIR - RRED) / (RNIR + RRED) \quad (3)$$

Here, RNIR represents the reflectance in the NIR band, and RRED represents the reflectance in the red band.

The Soil Adjusted Vegetation Index (SAVI) was developed by Huete [21] and Huete [22] to address noise present in NDVI due to canopy background and atmospheric conditions. SAVI incorporates an adjustment factor and is useful for correcting soil brightness and atmospheric effects [23];

$$SAVI = ((RNIR - RRED) / (RNIR + RRED + L)) \times (1 + L) \quad (4)$$

In Equation (4), L represents the adjustment factor, typically set to 0.5.

The Atmospheric Resistant Vegetation Index 2 (ARVI2) is designed to be resistant to atmospheric effects and sensitive to a wide range of chlorophyll concentrations. It is influenced by vegetation fraction and the rate of absorption of photosynthetic solar radiation. Equation (5) represents the calculation for ARVI2 [24,25]:

$$ARVI2 = -0.18 + 1.17 \times (RNIR - RRED / RNIR + RRED) \quad (5)$$

The Green-Near Infrared (G-NIR) index combines the green and near-infrared reflectance values to assess plant vigor and characterize vegetation structure. It has shown potential for discriminating between vegetation affected by oil spills and unaffected sites [26,27]:

$$G\text{-}NIR = (RGREEN - RNIR) / (RGREEN + RNIR) \quad (6)$$

In Equation (6), RGREEN represents the reflectance in the green band.

The Green-Short-Wave Infrared (G-SWIR) index has the ability to predict and sense nitrogen levels in plants [28] and can discriminate the moisture content of soil and vegetation. It may be useful for detecting changes in vegetation affected by oil spills [29]:

$$G\text{-}SWIR = (RGREEN - RSWIR) / (RGREEN + RSWIR) \quad (7)$$

In Equation (7), RSWIR represents the reflectance in the short-wave infrared (SWIR) band.

These equations and indices play crucial roles in analyzing satellite imagery and extracting valuable information about vegetation and environmental conditions.

3. Results and discussion

3.1 Assessment of oil spill's impact on the environment

The assessment of an oil spill's impact Joinkrama 4 and Akinima utilized the NDVI. **Tables 1 and 2** presented a comparison of NDVI spectral reflectance values between the oil spill site and a non-oil spill site. The results in **Figure 2** indicated the presence of unhealthy plants in the spill-affected area. The results revealed that the NDVI spectral reflectance values at the oil spill site were lower, indicating damage to the vegetation. **Figure 3** depicted the spectral reflectance, further emphasizing the significant extent of damage caused by the spill. The Oil Spill Site (OSS) exhibited a range of 0.0665 to 0.2622, while the Non-Oil Spill Site (NOSS) had a value of 0.4522. These findings demonstrate that the oil spill had a substantial adverse impact on the studied area's vegetation, as evidenced by the lower NDVI values and the presence of unhealthy plant growth.

The resulting SAVI values are then compared with historical data or a control area to identify regions where vegetation cover has been affected by the oil spill. SAVI proves effective in detecting oil spills because it provides a quantitative measure of the extent of the damage caused. The provided information indicates a negative impact on vegetation in the affected area due to the oil spill. Comparisons of SAVI values between the oil spill site and a non-oil spill site, as shown in **Tables 1 and 2**, further support the evidence of spill-induced damage in **Figure 4**. Spectral reflectance data in **Figure 5** illustrates that the oil spill site exhibits a lower SAVI range of 0.0333 to 0.1311, while the non-oil spill site displays a higher value of 0.2261. This disparity suggests that vegetation in the oil spill site is less healthy

compared to the non-oil spill site. Therefore, the presented information strongly indicates a significant negative impact of the oil spill on the vegetation in the affected area.

The study examined the health of vegetation in two distinct areas, one affected by an oil spill and the other untouched, using the Atmospheric Resistant Vegetation Index (ARVI). The analysis, presented in **Tables 1 and 2**, along with **Figure 6**, indicated the condition of vegetation in these areas. The color-coded images demonstrated that the regions affected by the oil spill exhibited unhealthy vegetation, while the non-oil spill area showed moderate vegetation. **Tables 1 and 2** were utilized to compare the ARVI values between the oil spill site and the non-oil spill site. The results derived from these tables were then used to generate **Figure 7**, which depicted the spectral reflectance of the oil spill site (OSS) and the non-oil spill site (NOSS). The range of the OSS values, ranging from –0.1022 to 0.1268, indicated the extent of vegetation damage caused by the oil spill. In comparison, the NOSS value of 0.3492 provided a reference point for evaluating the impact of the oil spill on vegetation in the area.

A comprehensive investigation of the influence of oil spills on vegetation stress through spectral reflectance in GNIR bands was conducted, as evident from the findings presented in **Tables 1 and 2** and **Figure 8**. These data depict the pre- and post-oil spill GNIR results, illustrating that the spills have induced stress and harm to the vegetation, resulting in changes in reflectance in both the green and NIR spectral bands. Moreover, the comparison of spectral reflectance between the oil spill site (OSS) and the non-oil spill site (NOSS) in **Figure 9**, provides further insights. The results demonstrate that reflectance values in the OSS range from –0.0479 to –0.1980, while the NOSS exhibits a reflectance of –0.3823. This comparison signifies that the presence of oil spills within the area significantly impacts the health of vegetation, leading to detectable changes in spectral reflectance that can be closely monitored. Consequently, the study underscores the significance of employing GNIR spectral reflectance as a means to identify and monitor the effects of oil spills on vegetation health. This knowledge can aid in the development of effective strategies to mitigate the damage caused by such incidents.

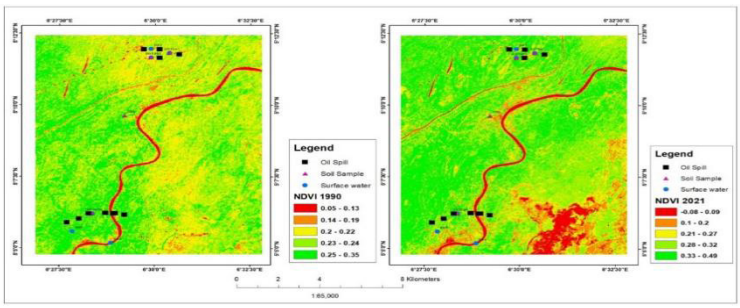

Figure 2. Vegetation analysis of normalized difference vegetation index (NDVI) 1990 and 2021.

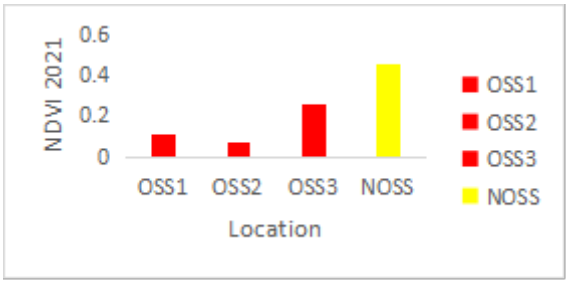

Figure 3. Normalized difference vegetation index for OSS and NOSS 2021.

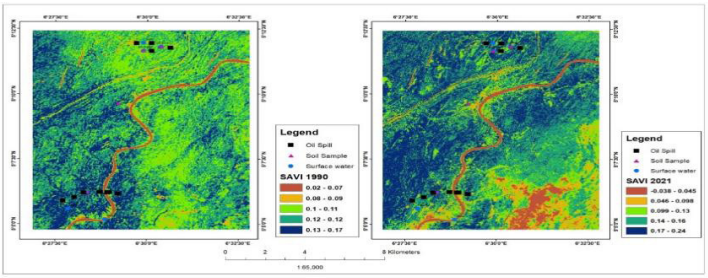

Figure 4. Vegetation analysis of soil adjusted vegetation index (SAVI) 1990 and 2021.

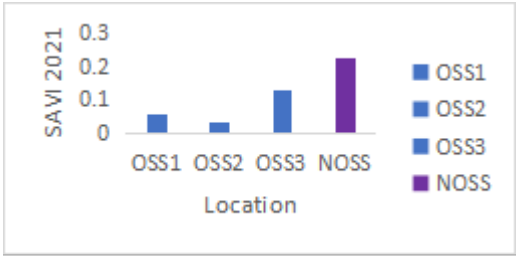

Figure 5. Vegetation analysis of soil adjusted vegetation index (SAVI) for OSS and NOSS 2021.

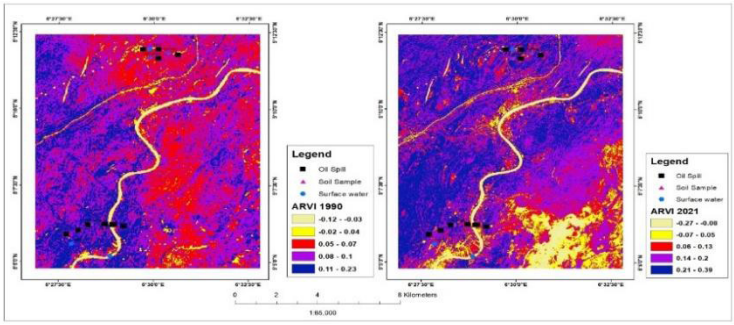

Figure 6. Vegetation analysis of atmospheric resistant vegetation index (ARVI) 1990 and 2021.

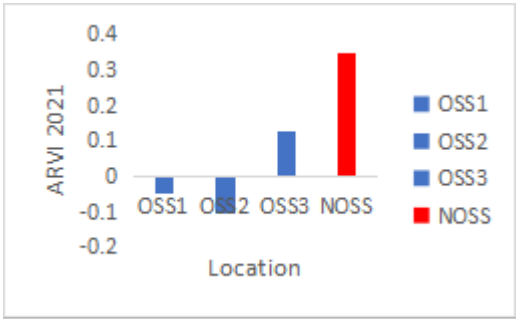

Figure 7. Vegetation analysis of atmospheric resistant vegetation index (ARVI) for OSS and NOSS 2021.

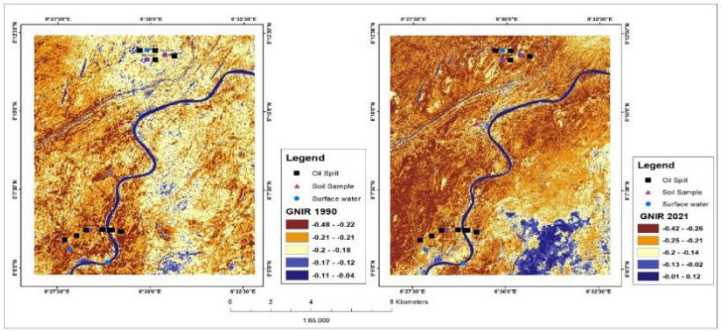

Figure 8. Vegetation analysis of green-near infrared (GNIR) 1990 and 2021.

Figure 9. Vegetation analysis of green-near infrared (GNIR) for OSS and NOSS 2021.

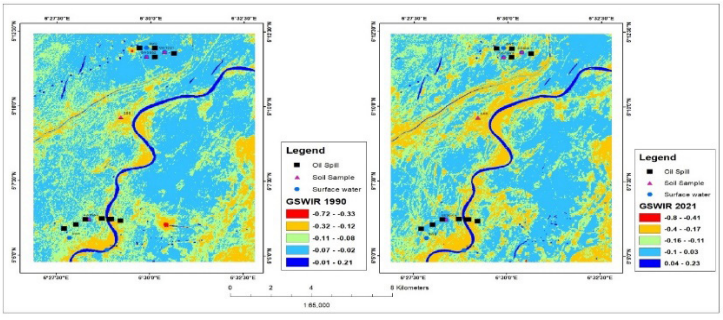

Figure 10. Vegetation analysis of green short wave infrared (GSWIR) 1990 and 2021.

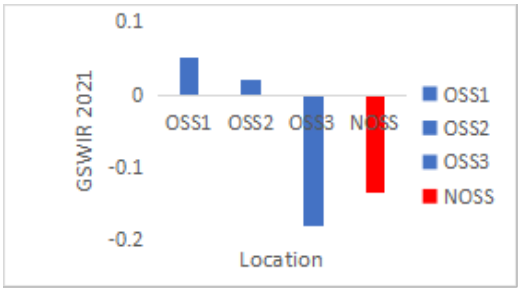

Figure 11. Vegetation analysis of green short wave infrared (GSWIR) for OSS and NOSS 2021.

The findings presented in **Tables 1 and 2** demonstrate the primary objective of the study, which was to evaluate how oil spills influence the well-being of vegetation by analyzing the spectral reflectance within the Green Short Wave Infrared (GSWIR) range. **Figure 10** reveals changes in GSWIR reflectance before and after the oil spill, indicating that the presence of the spill causes stress and harm to the vegetation, as evidenced by the altered reflectance. **Tables 4 and 5** compare the GSWIR reflectance between the oil spill site (OSS) and the non-oil spill site (NOSS). **Figure 11** illustrates that OSS 1 to OSS3 exhibit a range of values from 0.05717 to –0.1803, with OSS3 having a higher value than NOSS (–0.3823). This suggests that the presence of an oil spill has adversely affected the health of the vegetation in the area, resulting in changes in spectral reflectance in the Short Wave Infrared (SWIR) range. Thus, the study employed GSWIR spectral reflectance as a means to detect and monitor the impact of oil spills on vegetation health. The results underscore the necessity for effective measures to prevent oil spills and minimize their detrimental consequences on the environment.

Table 1. Vegetation indices spectral reflectance during the spill in soil sample 2021.

CODE	NDVI 2021	ARVI 2021	SAVI 2021	GSWIR 2021	GNIR 2021
OSS1	0.1115	–0.0495	0.0558	0.0517	–0.0479
OSS2	0.0665	–0.1022	0.0333	0.0214	–0.0104
OSS3	0.2622	0.1268	0.1311	–0.1803	–0.1980

Note: Oil spill site = OSS.

Table 2. Vegetation indices spectral reflectance in non-oil spill site 2021.

Vegetation indices	NOSS
NDVI	0.4523
ARVI	0.3492
SAVI	0.2261
GSWIR	–0.1332
GNIR	–0.3823

Note: Non-oil spill site = NOSS.

3.2 Pearson correlation coefficient analysis

Table 3 presents the findings of the Pearson correlation coefficient analysis, illustrating the relationship between various vegetation indices prior to and during an oil spill occurrence. The Pearson correlation coefficient assesses the linear connection between two variables and ranges from –1 (indicating a perfect negative correlation) to +1 (indicating a perfect positive correlation), with 0 representing no correlation. Based on the information provided, the Normalized Difference Vegetation Index (NDVI), Atmospheric Resistant Vegetation Index (ARVI), and Soil Adjusted Vegetation Index (SAVI) exhibit a strong positive correlation of r = 0.9229 before and during the oil spill event. This implies that these indices are highly associated and move in the same direction, suggesting their utility in monitoring vegetation changes during and after an oil spill. The statement further notes that the Green Short Wave Infrared (GSWIR) index demonstrates a strong positive correlation of r = 0.7559 before and during the oil spill event. Although this correlation is not as robust as the aforementioned indices, it still signifies a positive relationship between the variables. Lastly, the Green Near Infrared (GNIR) index reveals a strong positive correlation of r = 0.93649 before and during the oil spill event. This indicates a high correlation between GNIR and the other vegetation indices, making it suitable for monitoring vegetation changes throughout an oil spill event. Consequently, these correlations suggest that by combining different vegetation indices, one can effectively monitor vegetation changes before, during, and after an oil spill occurrence.

Table 3. Pearson correlation coefficient between vegetation indices before the spill and during the spill.

Vegetation indices before spill (1990) and during spill (2021)	r	Strength	Direction
NDVI	0.9229	Strong	positive
ARVI	0.9229	Strong	positive
SAVI	0.9229	Strong	positive
GSWIR	0.7559	Strong	positive
GNIR	0.9364	Strong	positive

The results from **Tables 4-7** indicate that there is a significant correlation between the Normalized

Difference Vegetation Index (NDVI) and the environmental parameters TPH, THC, and PAH in the affected oil spill site. Specifically, the results show a strong negative correlation (r = –0.7065) between NDVI and TPH, a strong positive correlation (r = 0.6968) between NDVI and THC, and a strong positive correlation (r = 0.5827) between NDVI and PAH. These correlations suggest that as the levels of TPH increase, the NDVI decreases, and as the levels of THC and PAH increase, the NDVI increases. This could indicate that higher levels of TPH negatively impact vegetation, while higher levels of THC and PAH positively impact vegetation in this particular oil spill site. However, it is important to note that correlation does not necessarily imply causation, and further research is needed to understand the specific mechanisms behind these relationships. Nonetheless, these findings could have important implications for understanding and mitigating the impacts of oil spills on vegetation in affected areas.

Table 4. Hydrocarbon results in soil.

Sample code	TPH	THC	PAH
Soil 1 (topsoil)	1.693	4.8	0.045
Soil 2 (topsoil)	1.736	4.1	0.03
Soil 3(topsoil)	1.691	4.82	0.043

Table 5. Pearson correlation coefficient between vegetation indices and TPH (topsoil).

2021	r	Strength	Direction
NDVI vs TPH	–0.7065	Strong	Negative
ARVI vs TPH	–0.7065	Strong	Negative
SAVI vs TPH	–0.7064	Strong	Negative
GSWIR vs TPH	0.4283	Weak	Positive
GNIR vs TPH	0.6840	Strong	Positive

Table 6. Pearson correlation coefficient between vegetation indices and THC (topsoil).

2021	r	Strength	Direction
NDVI vs THC	0.6958	Strong	Positive
ARVI vs THC	0.6958	Strong	Positive
SAVI vs THC	0.6958	Strong	Positive
GSWIR vs THC	–0.4147	Weak	Negative
GNIR vs THC	–0.6730	Strong	Negative

Table 7. Pearson correlation coefficient between vegetation indices and PAH (topsoil).

2021	r	Strength	Direction
NDVI vs PAH	0.5827	Strong	Positive
ARVI vs PAH	0.5827	Strong	Positive
SAVI vs PAH	0.5827	Strong	Positive
GSWIR vs PAH	–0.2765	Weak	Negative
GNIR vs PAH	–0.5570	Strong	Negative

3.3 T-test result for vegetation indices between the Oil Spill Site (OSS) and Non-Oil Spill Site (NOSS)

A dependent t-test was performed to compare the Normalized Difference Vegetation Index (NDVI) spectral reflectance between the Oil Spill Site (OSS) and Non-Oil Spill Site (NOSS), as indicated in **Table 8**. The results demonstrated a statistically significant difference between the two sites, with the NOSS mean surpassing the OSS mean. The t-test was conducted with a significance level (alpha) of $p < 0.05$, and the assumption of normally distributed difference scores was confirmed. The mean NDVI spectral reflectance for OSS was M = 0.1467 with a standard deviation of SD = 0.10250, while the mean for NOSS was M = 4.523 with a standard deviation of SD = 0.0000. The effect size was considered large, with d = 2.98, indicating a strong practical significance. Therefore, the findings imply that the presence of an oil spill negatively impacted vegetation health, resulting in lower NDVI spectral reflectance at the Oil Spill Site (OSS) compared to the Non-Oil Spill Site (NOSS). These results underscore the necessity for effective measures to prevent oil spills and minimize their environmental impact.

In **Table 9**, the results of a dependent t-test investigating the differences in the Atmospheric Resistant Vegetation Index (ARVI) between the Oil Spill Site (OSS) and Non-Oil Spill Site (NOSS) were presented. The research hypothesis aimed to determine whether the means of ARVI in OSS and NOSS were equal. The findings indicated a statistically significant difference between the mean ARVI scores of OSS and NOSS, with a t-value of 5.163 and a p-val-

ue less than 0.001. This suggests that the disparity between the means is unlikely to occur by chance. Furthermore, the effect size (d) was calculated as 2.98, demonstrating a substantial degree of practical significance. Thus, the results indicate that the mean ARVI for NOSS is significantly higher than the mean for OSS. It is important to note that the assumption of normally distributed difference scores was examined and met prior to conducting the analysis.

The data in **Table 10** show the results of a dependent t-test conducted to compare the Soil Adjusted Vegetation Index (SAVI) spectral reflectance at an Oil Spill Site (OSS) and a Non-Oil Spill Site (NOSS). The mean SAVI for OSS was 0.0734 with a standard deviation of 0.05122, while the mean SAVI for NOSS was 0.02261 with a standard deviation of 0.0000. The results of the dependent t-test indicated a statistically significant difference between the SAVI values for the OSS and NOSS ($t(3) = 5.164$, $p < 0.001$). The effect size was reported as large ($d = 2.98$), signifying a strong practical significance. Prior to conducting the t-test, it was confirmed that the assumption of normally distributed difference scores was satisfied. This assumption is crucial for the validity of the t-test results. Furthermore, an alpha level of $p < 0.05$ was employed, which is a common significance level in statistical testing. Consequently, the results suggest that the SAVI values were significantly higher at NOSS compared to OSS, indicating a potential discrepancy in vegetation health between the two sites.

Table 11 presents the outcome of a dependent t-test comparing the Green Short Wave Infrared (GSWIR) spectral reflectance at an Oil Spill Site (OSS) and a Non-Oil Spill Site (NOSS). The mean GSWIR for OSS was –0.0347 with a standard deviation of 0.07281, whereas the mean GSWIR for NOSS was –0.1332 with a standard deviation of 0.0000. The dependent t-test revealed a statistically significant difference between the SWIR values for OSS and NOSS ($t(3) = –1.34$, $p < 0.001$). The effect size was reported as large ($d = 0.77$), indicating a weak practical significance. It is noteworthy that the assumption of normally distributed difference scores was examined and satisfied prior to conducting the t-test. This assumption is critical for the validity of the t-test results. Additionally, an alpha level of $p < 0.05$ was employed, which is a common level of significance in statistical testing. Overall, the results suggest that the GSWIR values were significantly higher at NOSS compared to OSS, suggesting a potential disparity in the presence of oil or other contaminants between the two sites. However, the effect size was weak, implying that the practical significance of the difference might not be substantial.

The results depicted in **Table 12** demonstrate the use of a dependent t-test to examine the differences in Green Near Infrared (GNIR) spectral reflectance between an Oil Spill Site (OSS) and a Non-Oil Spill Site (NOSS). The findings indicated a statistically significant difference between OSS and NOSS, with a t-value of –5.180 and a p-value less than 0.001. This implies that the NOSS mean was significantly higher than the OSS mean for GNIR. The effect size was also computed, yielding a large effect size of $d = 3.0$. This indicates a strong degree of practical significance between the two groups. Prior to conducting the analysis, the assumption of normally distributed difference scores was examined, and the skew and kurtosis levels were found to be –1.46 and 0.00, respectively. These values were within the acceptable range for a t-test (i.e., skew < |2.0| and kurtosis < |9.0|; posten 1984), confirming the satisfaction of the assumption of normally distributed difference scores. Therefore, the results suggest a significant difference in GNIR spectral reflectance between OSS and NOSS, with NOSS exhibiting a higher mean than OSS.

4. Conclusions

The assessment of an oil spill's impact on vegetation in a specific area, utilizing the Normalized Difference Vegetation Index (NDVI), Atmospheric Resistant Vegetation Index (ARVI), Soil Adjusted Vegetation Index (SAVI), Green Short Wave Infrared (GSWIR), and Green Near Infrared (GNIR) spectral reflectance, revealed a significant negative impact on the health of vegetation due to the oil spill. The

Table 8. Paired samples statistics and Test for NDVI.

	Mean	N	Std. deviation	Std. error mean	Skew	Kurtosis	t
NOSS	0.4523	3	0	0	1.36	0.0000	5.164
OSS	0.1467	3	0.1025	0.05918			

Table 9. Paired samples statistics and tests for ARVI.

	Mean	N	Std. deviation	Std. error mean	Skew	Kurtosis	t
NOSS	0.3492	3	0.00000	0.00000	1.36	0.0000	5.163
OSS	–0.0083	3	0.11993	0.06924			

Table 10. Paired samples statistics and tests for SAVI.

	Mean	N	Std. error mean	Skew	Kurtosis	t
NOSS	0.2261	3	0.00000	1.36	0.0000	5.164
OSS	0.0734	3	0.02957			

Table 11. Paired samples statistics and tests for SWIR.

	Mean	N	Std. deviation	Std. error mean	Skew	Kurtosis	t
NOSS	–0.1332	3	0.00000	0.00000	–1.62	0.0000	–1.339
OSS	–0.0357	3	0.12611	0.07281			

Table 12. Paired samples statistics and tests for GNIR.

	Mean	N	Std. deviation	Std. error mean	Skew	Kurtosis	t
NOSS	–0.3823	3	0.00000	0.00000	–1.46	0.0000	–5.180
OSS	–0.0854	3	0.09927	0.05731			

comparisons between the oil spill site (OSS) and non-oil spill site (NOSS) consistently demonstrated lower vegetation health and damage in the OSS. The color-coded representations and spectral reflectance data provided visual evidence of unhealthy and stressed vegetation in the spill-affected area. The results from various statistical analyses, including dependent t-tests and Pearson correlation coefficients, further supported the findings by showing significant differences and relationships between vegetation indices and environmental parameters. Overall, the comprehensive findings suggest that the oil spill had a substantial adverse impact on the vegetation in the affected area. The lower values of NDVI, ARVI, SAVI, GSWIR, and GNIR reflectance at the oil spill site indicate damage and stress to the vegetation, while the healthier vegetation and higher reflectance values at the non-oil spill site serve as a reference point for comparison. The correlations between vegetation indices and environmental parameters provide insights into the relationship between oil spill characteristics and vegetation health. These findings highlight the importance of monitoring and mitigating the impacts of oil spills on vegetation. By utilizing remote sensing techniques and spectral reflectance analysis, it becomes possible to detect and monitor the extent of damage caused by oil spills. This knowledge can aid in the development of effective strategies for preventing and minimizing the detrimental consequences of oil spills on the environment and vegetation in affected areas.

Author Contributions

J. L.E developed the study, processed the data, and assisted with part of the writing, while E.E.D. assisted with writing and formatting. The final version was co-written by all authors.

Conflict of Interest

There is no conflict of interest.

References

[1] Okpobiri, O., Harry, A.A., 2022. Monitoring and detecting the impact of oil sabotage on land using multispectral imagery. International Journal of Multidisciplinary Research and Publications (IJMRAP). 4(9), 66-74.

[2] Kadafa, A.A., 2012. Oil exploration and spillage in the Niger Delta of Nigeria. Civil and Environmental Research. 2(3), 38-51.

[3] Okonkwo, C.N.P., Kumar, L., Taylor, S., 2015. The Niger Delta wetland ecosystem: What threatens it and why should we protect it? African Journal of Environmental Science and Technology. 9(5), 451-463.
DOI: https://doi.org/10.5897/AJEST2014.1841

[4] Environmental Assessment of Ogoniland [Internet]. Available from: http://www.zaragoza.es/contenidos/medioambiente/onu/issue06/1130-eng-sum.pdf

[5] Oyem, A., (2001). Christian call for action on Nigerian oil spill. Sage-Oxford's Christian Environmental Group.

[6] Egirani, D.E., Shehata, N., Ugwu, I.M., et al., 2021. Exposure, geochemical, and spatial distribution patterns of an oil spill in parts of the Niger Delta Region of Nigeria. Health and Environment. 2(1), 103-117.
DOI: https://doi.org/10.25082/HE.2021.01.005

[7] Egobueze, F.E., Rowland, E.D., Ebizimo, D.S., 2022. Multispectral imagery for detection and monitoring of vegetation affected by oil spills and migration pattern in Niger Delta Region, Nigeria. World Journal of Advanced Research and Reviews. 15(1), 447-458.
DOI: https://doi.org/10.30574/wjarr.2022.15.1.0682

[8] Van der Werff, H., Van der Meijde, M., Jansma, F., et al., 2008. A spatial-spectral approach for visualization of vegetation stress resulting from pipeline leakage. Sensors. 8(6), 3733-3743.
DOI: https://doi.org/10.3390/s8063733

[9] Guyot, G., Baret, F., Jacquemoud, S., 1992. Imaging spectroscopy for vegetation studies. Kluwer Academic Publishers: Dordrecht. pp. 145-165.

[10] Rowland, E.D., Okpobiri, O., 2021. Floodplain mapping and risks assessment of the Orashi River using remote sensing and GIS in the Niger Delta Region, Nigeria. Journal of Geographical Research. 4(2), 10-16.
DOI: https://doi.org/10.30564/jgr.v4i2.3014

[11] Rayment, R.A., 1965. Aspects of the geology of Nigeria—The stratigraphy of the cretaceous and cenozoic deposits. Ibadan University Press: Ibadan.

[12] Reijers, T., 2011. Stratigraphy and sedimentology of the Niger Delta. Geologos. 17(3), 133-162.

[13] Short, K.C., Stauble, A.J., 1967. Outline of geology of Niger Delta. AAPG Bulletin. 51(5), 761-779.

[14] Adewoyin, O.O., Joshua, E.O., Akinwumi, I.I., et al., 2017. Evaluation of geotechnical parameters using geophysical data. Journal of Engineering and Technological Sciences. 49(1), 95-113.

[15] Etu–Efeotor, J.O., 1997. Fundamentals of petroleum geology. Paragraphic: Port Harcourt.

[16] Jiang, Z., Huete, A.R., Didan, K., et al., 2008. Development of a two-band enhanced vegetation index without a blue band. Remote Sensing of Environment. 112(10), 3833-3845.
DOI: https://doi.org/10.1016/j.rse.2008.06.006

[17] Chavez, P.S., 1996. Image-based atmospheric corrections-revisited and improved. Photogrammetric Engineering and Remote Sensing. 62(9), 1025-1035.

[18] Rowland, E.D., Omonefe, F., 2022. Environmental monitory and impact assessment of solid waste dumpsite using multispectral imagery in Yenagoa, Bayelsa state, Nigeria. International Journal of Environmental Science and Technology. 19(2), 1007-1024.
DOI: https://doi.org/10.1007/s13762-021-03456-2

[19] Rouse, J.W.Jr., Haas, R.H., Schell, J.A., et al., 1973. Monitoring the Vernal Advancement and Retrogradation (Green Wave Effect) of Natural

Vegetation [Internet]. Available from: https://ntrs.nasa.gov/citations/19750020419

[20] Running, S.W., Justice, C.O., Salomonson, V., et al., 1994. Terrestrial remote sensing science and algorithms planned for EOS/MODIS. International Journal of Remote Sensing. 15(17), 3587-3620.
DOI: https://doi.org/10.1080/01431169408954346

[21] Huete, A.R., 1988. A soil-adjusted vegetation index (SAVI). Remote Sensing of Environment. 25(3), 295-309.

[22] Huete, A.R., Hua, G., Qi, J., et al., 1992. Normalization of multidirectional red and NIR reflectances with the SAVI. Remote Sensing of Environment. 41(2-3), 143-154.
DOI: https://doi.org/10.1016/0034-4257(92)90074-T

[23] Rondeaux, G., Steven, M., Baret, F., 1996. Optimization of soil-adjusted vegetation indices. Remote Sensing of Environment. 55(2), 95-107.
DOI: https://doi.org/10.1016/0034-4257(95)00186-7v

[24] Gitelson, A.A., Kaufman, Y.J., Merzlyak, M.N., 1996. Use of a green channel in remote sensing of global vegetation from EOS-MODIS. Remote sensing of Environment. 58(3), 289-298.
DOI: https://doi.org/10.1016/S0034-4257(96)00072-7

[25] Kaufman, Y.J., Tanre, D., 1992. Atmospherically resistant vegetation index (ARVI) for EOS-MODIS. IEEE Transactions on Geoscience and Remote Sensing. 30(2), 261-270.
DOI: https://doi.org/10.1109/36.134076

[26] Sripada, R.P., Heiniger, R.W., White, J.G., et al., 2006. Aerial color infrared photography for determining early in-season nitrogen requirements in corn. Agronomy Journal. 98(4), 968-977.
DOI: https://doi.org/10.2134/agronj2005.0200

[27] Adamu, B., Tansey, K., Ogutu, B., 2015. Using vegetation spectral indices to detect oil pollution in the Niger Delta. Remote Sensing Letters. 6(2), 145-154.
DOI: https://doi.org/10.1080/2150704x.2015.1015656

[28] Herrmann, I., Karnieli, A., Bonfil, D.J., et al., 2010. SWIR-based spectral indices for assessing nitrogen content in potato fields. International Journal of Remote Sensing. 31(19), 5127-5143.
DOI: https://doi.org/10.1080/01431160903283892

[29] Karnieli, A., Kaufman, Y.J., Remer, L., et al., 2001. AFRI—Aerosol free vegetation index. Remote Sensing of Environment. 77(1), 10-21.
DOI: https://doi.org/10.1016/S0034-4257(01)00190-0